

Unquenched Gluon Propagator in Landau Gauge

Patrick O. Bowman,^{1,2} Urs M. Heller,³ Derek B. Leinweber,¹ Maria B. Parappilly,¹ and Anthony G. Williams¹

¹*Special Research Centre for the Subatomic Structure of Matter and
The Department of Physics, University of Adelaide, SA 5005, Australia*

²*Nuclear Theory Center, Indiana University, Bloomington IN 47405, USA*

³*American Physical Society, One Research Road, Box 9000, Ridge NY 11961-9000, USA*

(Dated: February 17, 2004)

Using lattice quantum chromodynamics (QCD) we perform an unquenched calculation of the gluon propagator in Landau gauge. We use configurations generated with the AsqTad quark action by the MILC collaboration for the dynamical quarks and compare the gluon propagator of quenched QCD (*i.e.*, the pure Yang-Mills gluon propagator) with that of 2+1 flavor QCD. The effects of the dynamical quarks are clearly visible and lead to a significant reduction of the nonperturbative infrared enhancement relative to the quenched case.

PACS numbers: PACS numbers: 12.38.Gc 11.15.Ha 12.38.Aw 14.70.Dj

I. INTRODUCTION

The gluon propagator, the most basic quantity of QCD, has been subject to much calculation and speculation since the origin of the theory. In particular there has long been interest in the infrared behavior of the Landau gauge gluon propagator as a probe into the mechanism of confinement [1]. Some authors have argued it to be infrared finite [2, 3, 4] while others favored infrared singular [5, 6]. There is a long history of its study on the lattice, in quenched QCD [7, 8, 9, 10, 11, 12, 13, 14, 15, 16, 17, 18, 19] and in quenched $SU(2)$ [20, 21]. The restriction to quenched lattice gauge theory calculations has been due to the lack of sufficient computational resources. The quenched theory differs from full QCD only in the relative weighting of the background gauge configurations (due to the fermion determinant), but the evaluation of the Green's functions is otherwise the same. In the quenched approximation the fermion determinant is replaced by unity and this corresponds to the complete suppression of all quark loops. The removal of quark loops is equivalent to the limit where all sea-quark masses are taken to infinity. In this paper, we report the first results for the gluon propagator from an unquenched lattice computation.

We study the gluon propagator in Landau gauge using configurations generated by the MILC collaboration [22] available from the Gauge Connection [27]. These use “AsqTad” improved staggered quarks, giving us access to relatively light sea quarks. We find that the addition of dynamical quarks preserves the qualitative features of the gluon dressing function $q^2 D(q^2)$ in the quenched case – enhancement for intermediate infrared momenta followed by suppression in the deep infrared – but produces a clearly visible effect. A significant suppression of the infrared enhancement with respect to the quenched case is observed. It is interesting to compare these results to those of a recent Dyson-Schwinger equation study [23].

II. DETAILS OF THE CALCULATION

The gluon propagator is gauge dependent and we work in the Landau gauge for ease of comparison with other studies. It is also the simplest covariant gauge to implement on the lattice. Landau gauge is a smooth gauge that preserves the Lorentz invariance of the theory, so it is a popular choice. It will be interesting to repeat this calculation for the Gribov-copy free Laplacian gauge, but that will be left for a future study.

The MILC configurations were generated with the $\mathcal{O}(a^2)$ one-loop Symanzik improved [24] Lüscher–Weisz gauge action [25]. The dynamical configurations use the “AsqTad” quark action, an $\mathcal{O}(a^2)$ Symanzik improved staggered fermion action. β and the bare sea-quark masses are matched such that the lattice spacing is held constant. The lattices we consider all have the same dimensions. This means that all systematics are fixed; the only variable is the addition of quark loops. The parameters are summarized in Table I. The lattice spacing is approximately 0.125 fm [26].

In Landau gauge the gluon propagator is entirely transverse. In Euclidean space, in the continuum, the gluon

TABLE I: Lattice parameters used in this study. The dynamical configurations each have two degenerate light quarks (up/down) and a heavier quark (strange). In physical units the bare masses range from ~ 16 MeV to ~ 79 MeV. The lattice spacing is $a \simeq 0.125$ fm.

	Dimensions	β	Bare Quark Mass	# Configurations
1	$20^3 \times 64$	8.00	quenched	192
2	$20^3 \times 64$	6.76	0.01, 0.05	193
3	$20^3 \times 64$	6.79	0.02, 0.05	249
4	$20^3 \times 64$	6.81	0.03, 0.05	212
5	$20^3 \times 64$	6.83	0.04, 0.05	337

propagator has the tensor structure

$$D_{\mu\nu}(q) = \left(\delta_{\mu\nu} - \frac{q_\mu q_\nu}{q^2} \right) D(q^2), \quad (1)$$

and at tree-level,

$$D(q^2) = \frac{1}{q^2}. \quad (2)$$

With this lattice gauge action the propagator at tree-level is

$$D^{-1}(p_\mu) = \frac{4}{a^2} \sum_\mu \left\{ \sin^2 \left(\frac{p_\mu a}{2} \right) + \frac{1}{3} \sin^4 \left(\frac{p_\mu a}{2} \right) \right\}, \quad (3)$$

where

$$p_\mu = \frac{2\pi n_\mu}{aL_\mu}, \quad n_\mu \in \left(-\frac{L_\mu}{2}, \frac{L_\mu}{2} \right], \quad (4)$$

a is the lattice spacing and L_μ is the length of the lattice in the μ direction. As explained in Ref. [14], this suggests a “kinematic” choice of momentum,

$$q_\mu(p_\mu) \equiv \frac{2}{a} \sqrt{\sin^2 \left(\frac{p_\mu a}{2} \right) + \frac{1}{3} \sin^4 \left(\frac{p_\mu a}{2} \right)}, \quad (5)$$

ensuring that the lattice gluon propagator has the correct tree-level behavior.

The bare gluon propagator, $D(q)$ is related to the renormalized propagator $D_R(q; \mu)$ through

$$D(q) = Z_3(\mu, a) D_R(q; \mu) \quad (6)$$

where μ is the renormalization point. In a renormalizable theory such as QCD, renormalized quantities become independent of the regularization parameter in the limit where it is removed. Z_3 is then defined by some renormalization prescription. We choose the momentum space subtraction (MOM) scheme where $Z_3(\mu, a)$ is determined by imposing the renormalization condition

$$D_R(q)|_{q^2=\mu^2} = \frac{1}{\mu^2}, \quad (7)$$

i.e. it takes the tree-level value at the renormalization point. In the following figures we have chosen $\mu = 4$ GeV.

III. SIMULATIONS RESULTS

Lattice studies strongly suggest that the quenched gluon propagator is infrared finite [14]. As is customary, we will begin by considering the (necessarily finite) gluon dressing function, $q^2 D(q^2)$. In Fig. 1 we compare the well-known quenched dressing function with that for 2+1 flavor QCD. For the moment we only consider the lightest of our dynamical quarks as we expect that they will show the greatest difference from the quenched case.

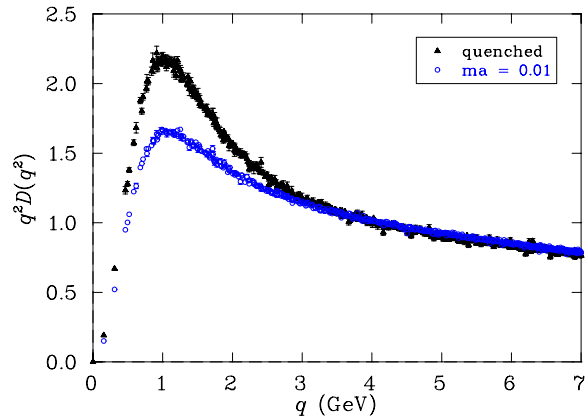


FIG. 1: Gluon dressing function in Landau gauge. Full triangles correspond to the quenched calculation, while open circles correspond to 2+1 flavor QCD. As the lattice spacing and volume are the same, the difference between the two results is entirely due to the presence of quark loops. The renormalization point is at $\mu = 4$ GeV. Data has been cylinder cut [16].

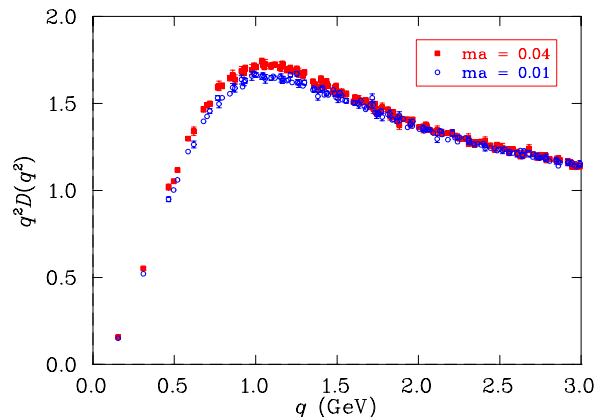


FIG. 2: The sea-quark mass dependence of the Landau gauge gluon propagator dressing function renormalized at $\mu = 4$ GeV. Filled squares correspond to u and d bare masses $\simeq 63$ MeV and bare s -quark mass $\simeq 79$ MeV. Open circles correspond to the same strange-quark mass, but with bare u and d masses $\simeq 16$ MeV. Data has been cylinder cut [16]. Increasing the sea-quark masses alters the results in the expected way, *i.e.* towards the quenched data.

Indeed there is a clear difference between quenched and dynamical quark behavior in the infrared region. The addition of quark loops to the gluon propagator softens the infrared enhancement without altering its basic features. The screening of dynamical sea quarks brings the 2 + 1 flavor results significantly closer to the tree-level form, $q^2 D(q^2) = 1$.

In Fig. 2 we show the gluon dressing function for the lightest and for the heaviest u and d quark masses in our

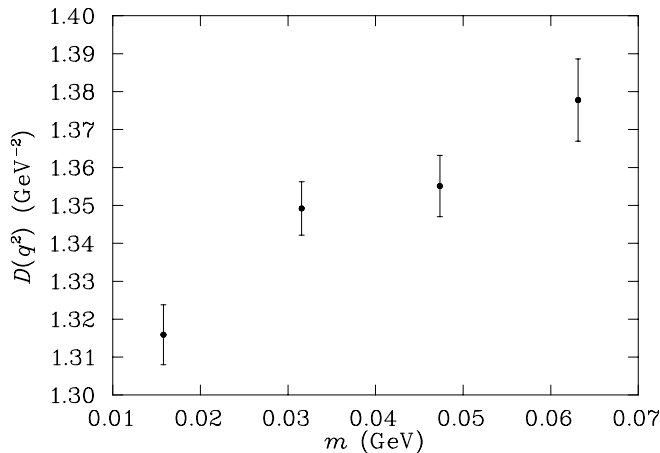


FIG. 3: The renormalized propagator at one momentum point in the infrared hump of the gluon dressing function ($q \simeq 1.12$ GeV) is shown here as a function of the bare light-quark mass.

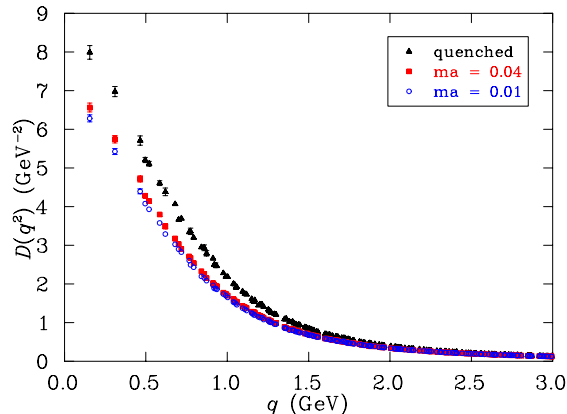


FIG. 4: The sea-quark mass dependence of the Landau gauge gluon propagator renormalized at $\mu = 4$ GeV. Filled triangles illustrate the quenched propagator while filled squares correspond to bare up/down masses $\simeq 63$ and bare strange-quark mass $\simeq 79$ MeV. Open circles correspond to lighter bare up/down masses $\simeq 16$ MeV but with the same strange quark mass. Data has been cylinder cut [16].

set. These correspond to bare light-quark masses of $\simeq 16$ MeV and $\simeq 63$ MeV respectively; a factor of four difference. The bare strange-quark mass is the same in both cases ($\simeq 79$ MeV). The mass dependence of the gluon dressing function is only just detectable. We expect that increasing the sea-quark masses further will interpolate between the curves in Fig. 1. We see that the gluon propagator changes in the expected way. As the sea-quark mass increases, the curve moves toward the quenched result. However, for the range of bare quark masses studied here the change is relatively small. This transition would be better studied with heavier sea quarks.

Another view of the mass dependence of the gluon propagator is provided in Fig. 3. We choose one data

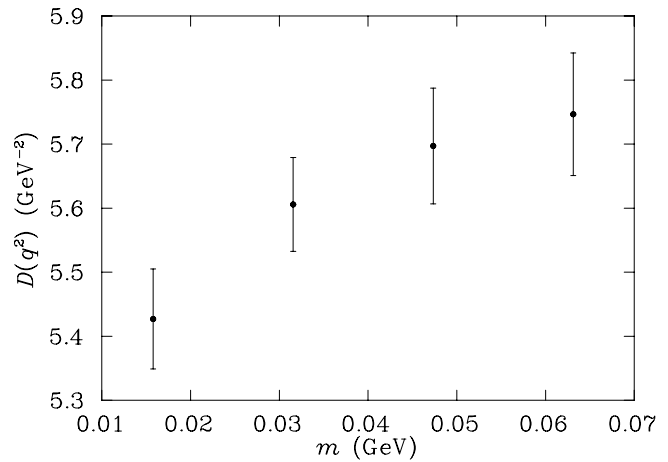


FIG. 5: The light sea-quark mass dependence of the renormalized gluon propagator at a momentum point in the infrared region ($q \simeq 0.31$ GeV).

point from the infrared hump ($q \simeq 1.12$ GeV) and plot it for each choice of bare light-quark mass. Although the variation in the propagator at this momentum is only 4.5% over the range of quark masses investigated here, the light sea-quark mass dependence is clearly resolved.

In Fig. 4 we present results for the gluon propagator, $D(q^2)$. The largest effects of unquenching are observed in the deep infrared. The shape of the curves suggest that previous results indicating the infrared-finite nature of the quenched gluon propagator [14] are unchanged upon unquenching. The results suggest that the gluon propagator of QCD is infrared finite. It will be interesting to examine the behavior of $D(0)$ as a function of volume to elucidate this aspect of the gluon propagator further.

Finally, in Fig. 5 the light sea-quark mass dependence of the renormalized gluon propagator is illustrated for a momentum point in the infrared region. To avoid finite volume artifacts, the second smallest nontrivial momentum is considered. Whereas the mass dependence of the propagator for the masses studied here is at the 4.5% level for $q \simeq 1.12$ GeV, the variance is larger in the infrared region at 6% for $q \simeq 0.31$ GeV.

IV. CONCLUSIONS

The addition of quark loops has a clear, quantitative effect on the gluon propagator. While its basic structure is qualitatively similar there is significant screening of the propagator in the infrared. As anticipated, the effect is to suppress the non-abelian enhancement of the gluon propagator in the nonperturbative infrared-momentum region. This is relevant to analytic studies of the gluon propagator and confinement [23]. Despite the clear difference between the quenched and dynamical results, we see little dependence on the dynamical quark mass for the range of available light sea-quark masses. The dependence that is observed is consistent with expectations.

Calculations on finer lattices are currently being made, which will provide more information on the ultraviolet nature of the propagator and provide a test for finite lattice spacing artifacts. We would like to extend the study to a wider range of dynamical masses to study both the chiral limit and the transition to the quenched limit. Finally, a study of the volume dependence of the propagator will provide valuable insights into the nature of the propagator at $q^2 = 0$.

ACKNOWLEDGMENTS

This research was supported by the Australian Research Council and by grants of time on the Hydra Supercomputer, supported by the South Australian Partnership for Advanced Computing.

-
- [1] J. E. Mandula, (1998), hep-lat/9907020.
 - [2] V. N. Gribov, Nucl. Phys. **B139**, 1 (1978).
 - [3] M. Stingl, Phys. Rev. **D34**, 3863 (1986).
 - [4] D. Zwanziger, Nucl. Phys. **B364**, 127 (1991).
 - [5] S. Mandelstam, Phys. Rev. **D20**, 3223 (1979).
 - [6] K. Buttner and M. R. Pennington, Phys. Rev. **D52**, 5220 (1995), hep-ph/9506314.
 - [7] J. E. Mandula and M. Ogilvie, Phys. Lett. **B185**, 127 (1987).
 - [8] C. W. Bernard, C. Parrinello, and A. Soni, Phys. Rev. **D49**, 1585 (1994), hep-lat/9307001.
 - [9] P. Marenzoni, G. Martinelli, and N. Stella, Nucl. Phys. **B455**, 339 (1995), hep-lat/9410011.
 - [10] J. P. Ma, Mod. Phys. Lett. **A15**, 229 (2000), hep-lat/9903009.
 - [11] D. Becirevic *et al.*, Phys. Rev. **D60**, 094509 (1999), hep-ph/9903364.
 - [12] D. Becirevic *et al.*, Phys. Rev. **D61**, 114508 (2000), hep-ph/9910204.
 - [13] H. Nakajima and S. Furui, Nucl. Phys. **A680**, 151 (2000), hep-lat/0004023.
 - [14] F. D. R. Bonnet, P. O. Bowman, D. B. Leinweber, A. G. Williams, and J. M. Zanotti, Phys. Rev. **D64**, 034501 (2001), hep-lat/0101013.
 - [15] K. Langfeld, H. Reinhardt, and J. Gattnar, Nucl. Phys. **B621**, 131 (2002), hep-ph/0107141.
 - [16] D. B. Leinweber, J. I. Skullerud, A. G. Williams, and C. Parrinello, Phys. Rev. **D60**, 094507 (1999), hep-lat/9811027.
 - [17] D. B. Leinweber, J. I. Skullerud, A. G. Williams, and C. Parrinello, Phys. Rev. **D58**, 031501 (1998), hep-lat/9803015.
 - [18] P. O. Bowman, U. M. Heller, D. B. Leinweber, and A. G. Williams, Phys. Rev. **D66**, 074505 (2002), hep-lat/0206010.
 - [19] F. D. R. Bonnet, P. O. Bowman, D. B. Leinweber, and A. G. Williams, Phys. Rev. **D62**, 051501 (2000), hep-lat/0002020.
 - [20] A. Cucchieri, Phys. Lett. **B422**, 233 (1998), hep-lat/9709015.
 - [21] A. Cucchieri, T. Mendes, and A. R. Taurines, Phys. Rev. **D67**, 091502 (2003), hep-lat/0302022.
 - [22] C. W. Bernard *et al.*, Phys. Rev. **D64**, 054506 (2001), hep-lat/0104002.
 - [23] R. Alkofer, W. Detmold, C. S. Fischer, and P. Maris, (2003), hep-ph/0309077.
 - [24] K. Symanzik, Nucl. Phys. **B226**, 187 (1983).
 - [25] M. Luscher and P. Weisz, Commun. Math. Phys. **97**, 59 (1985), Erratum-ibid. **98**, 433 (1985).
 - [26] HPQCD, C. T. H. Davies *et al.*, Phys. Rev. Lett. **92**, 022001 (2004), hep-lat/0304004.
 - [27] <http://www.qcd-dmz.nersc.gov>